Design, synthesis, and biological activity of synthetically-accessible analog of aplysiatoxin with (*R*)-(−)-carvone-based conformation-controlling unit

Yoshiyuki Suzuki[a], Keiichi Moritoki[a], Mizuki Kajiwara[a], Ryo C. Yanagita[b,*], Yasuhiro Kawanami[b], Yusuke Hanaki[b], and Kazuhiro Irie[c]

[a]Division of Applied Biological and Rare Sugar Sciences, Graduate School of Agriculture, Kagawa University, Kagawa 761-0795, Japan
[b]Department of Applied Biological Science, Faculty of Agriculture, Kagawa University, Kagawa 761-0795, Japan
[c]Division of Food Science and Biotechnology, Graduate School of Agriculture, Kyoto University, Kyoto 606-8502, Japan

Corresponding Author
*(R.C.Y.) E-mail: yanagita.ryo@kagawa-u.ac.jp
ORCID
Ryo C. Yanagita: 0000-0002-9217-5507

This is an Accepted Manuscript version of the following article, accepted for publication in *Bioscience, Biotechnology, and Biochemistry*.
Design, synthesis, and biological activity of synthetically-accessible analog of aplysiatoxin with (*R*)-(−)-carvone-based conformation-controlling unit
Yoshiyuki Suzuki, Keiichi Moritoki, Mizuki Kajiwara, Ryo C. Yanagita, Yasuhiro Kawanami, Yusuke Hanaki, and Kazuhiro Irie
Bioscience, Biotechnology, and Biochemistry, 2022, volume 86, issue 8, pages 1013–1023.
`https://doi.org/10.1093/bbb/zbac084`

Keywords: Protein kinase C; Aplysiatoxin; Simplified analog; Antiproliferative activity; Cyclic ketal

ABSTRACT

Simplified analogs of aplysiatoxin (ATX) such as 10-Me-aplog-1 exhibit potent antiproliferative activity toward human cancer cell lines by activating protein kinase C (PKC). However, the synthesis of 10-Me-aplog-1 involved a 23-step longest linear sequence (LLS). Therefore, we have been working toward the development of a more synthetically accessible analog of ATX. In this study, we designed a new analog of ATX wherein a cyclic ketal moiety derived from (*R*)-(−)-carvone replaced the spiroketal moiety in 18-deoxy-aplog-1. The new analog's synthesis proceeded in an eight-step LLS. Although the configuration at position 3 of the cyclic ketal in the (*R*)-(−)-carvone-based analog was opposite to those of ATX and 18-deoxy-aplog-1, the antiproliferative activity toward human cancer cell lines of the carvone-based analog was comparable to that of 18-deoxy-aplog-1. The obtained results indicate the potential of the carvone-based analog as a basis for discovering PKC-targeting molecules requiring a decreased number of synthetic steps.

1 INTRODUCTION

Members of the protein kinase C (PKC) enzyme family, which are serine/threonine kinases, play a crucial role in cell proliferation, differentiation, and apoptosis.[1,2] Since loss-of-function mutations of PKCs occur in many cancers, PKCs are assumed to act as tumor suppressors.[3] Thus, activation of PKCs could be an effective strategy in cancer therapy.[4] Naturally occurring tumor promoters, such as 12-O-tetradecanoylphorbol 13-acetate (TPA), teleocidin B-4, and aplysiatoxin (ATX, Figure 1), activate conventional PKCs (cPKC: α, βI, βII, γ) and novel PKCs (nPKC: δ, ε, η, θ) by binding to their C1A and C1B domains,[5–8] and the prolonged activation of PKCs results in the down-regulation and the loss of functional isozymes. Despite their tumor-promoting activity, these compounds have been observed to exhibit antiproliferative and proapoptotic activities toward cancer cell lines via PKC activation.[9] Another naturally occurring PKC activator, bryostatin-1 (Figure 1), has been attracting attention as a novel anticancer agent, because it displays antiproliferative activity toward several cancer cell lines, but it does not exhibit any tumor-promoting activity.[10] However, phase I and II clinical trials of bryostatin-1 revealed that bryostatin-1 alone or in combination with other chemotherapeutic agents was not effective in cancer patients.[11] Therefore, the development of PKC-activating anticancer seeds other than the bryostatin-1 skeleton is necessary.

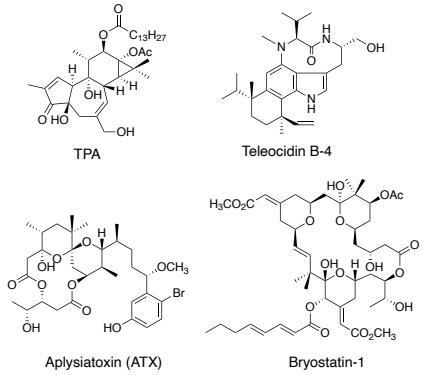

Figure 1: Structure of naturally occurring PKC activators.

Recently, Nakagawa and Irie *et al*. reported that aplogs (Figure 2), which are simplified analogs of ATX, exhibited antiproliferative activity, but they did not exhibit tumor-promoting and proinflammatory activities.[12,13] In particular, 10-Me-aplog-1 (Figure 2), which exhibited a potent antiproliferative activity that was comparable to that of ATX, is promising as an anticancer lead compound. However, its synthesis involved a 23-step longest linear sequence (LLS) with an overall yield of 1.1%.[14,15] Therefore, our group has tried to simplify or modify the structure of 10-Me-aplog-1 to shorten the mentioned synthetic pathway.

The spiroketal structure can be found in many natural products.[16] In ATX, a spiroketal moiety forces the macrolactone ring into its active conformation and provides sufficient hydrophobicity and bulkiness so that ATX forms a stable complex with phospholipid membranes. Therefore, substitution or modification of the spiroketal moiety is a challenge in the effort to obtain active analogs of ATX. Hayakawa et al. reported that compounds 1 and 2 (Figure 2), wherein an oxygen atom replaces the carbon atom at position 4 of 10-Me-aplog-1 to facilitate the construction of a spiro structure, exhibited antiproliferative activity inferior to those of 10-Me-aplog-1.[17] Moreover, the synthetic route leading to **1** and **2** still was characterized by an 18-step LLS, and a further decrease in the number of synthetic steps is needed. Kishi and coworkers previously reported that ATX analog **3** (Figure 2), in which a carbon atom replaces the oxygen atom of the B ring, retains the ability to activate PKCs,[18] indicating that substitution of the B ring with a cyclohexane ring does not impair the compound's activity. In the present study, we designed a novel analog **4**, wherein a cyclic ketal moiety derived from (*R*)-(−)-carvone replaces the spiroketal moiety of ATX. Analog **4** was synthesized in a relatively low number of steps (eight) and higher overall yield (1.8%) compared to the previously reported analogs. Carvone-based analog **4** exhibited similar antiproliferative activity and binding affinity toward PKC to other aplogs. Moreover, the synthetic route developed for the preparation of **4** allows the side-chain structure to be diversified. Thus, **4** could be a sound basis for synthesizing a wide range of ATX analogs.

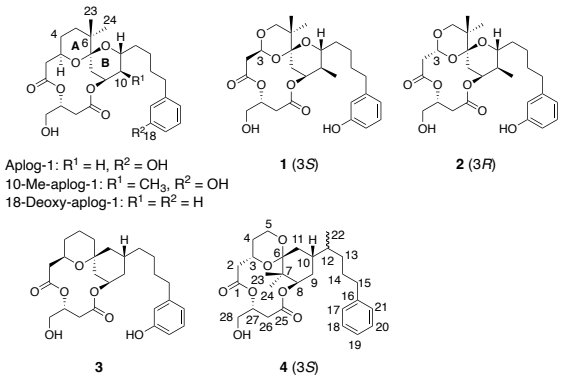

Figure 2: Structure of aplogs, simplified analogs of ATX.

2 RESULTS AND DISCUSSION

2.1 Design of 4

The spiroketal moiety of ATX acts as a conformation-controlling unit for a receptor-recognition domain, which includes a hydroxy group and two ester groups.[19–21] This study aimed to develop an ATX analog that

was more synthetically accessible than ATX by modifying 18-deoxy-aplog-1, a compound lacking the 10-methyl and phenolic hydroxy groups present in 10-Me-aplog-1. For this purpose, we planned to replace the positions of an oxygen atom in the B ring, a dimethylmethylene group at position 6, and a methylene group at position 8 in 18-deoxy-aplog-1, so as to obtain ATX analog **4** comprising a cyclic ketal: 7,7-dimethyl-1,5-dioxaspiro[5.5]undecane (Figure 3). Thus, by replacing a spiroketal with a cyclic ketal, we expected to achieve the efficient construction of the conformation-controlling unit from optically active (*R*)-(−)-carvone in association with a significant shortening of the number of synthetic steps. The *gem*-dimethyl group at position 7 was expected to shield the oxygen atom in the A ring effectively, thus providing the molecule with sufficient hydrophobicity to form hydrophobic interaction with the hydrophobic residues forming the binding cleft in the C1 domains and phospholipid bilayer. Note that the methyl group at position 12 in **4** derived from (*R*)-(−)-carvone also existed in ATX, and the reintroduction of this group into aplogs was observed to result in an increase in the antiproliferative activity and a decrease in the undesired proinflammatory activity.[22]

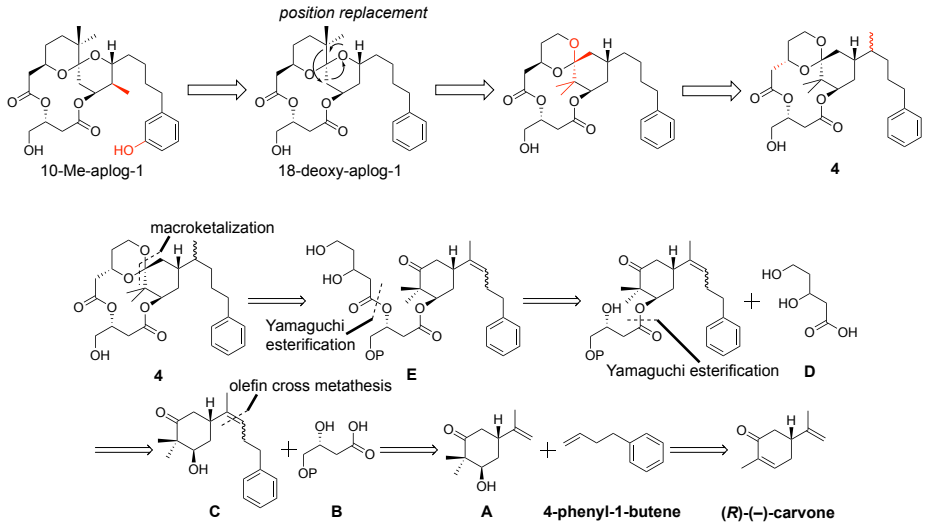

Figure 3: Analog design and retrosynthetic analysis of **4**.

Retrosynthetic analysis of **4** provided a convergent synthetic route (Figure 3), which involves macroketalization of an ester (**E**) and the formation of ester bonds between fragments **B**, **C**, and **D**. Olefin cross-metathesis with alcohol A introduces the side chain at position 10. The fragment **A** is accessible from (*R*)-(−)-carvone by a known method. In the macroketalization step, we anticipated that the steric hindrance of the 23-methyl group and the axial hydrogens at positions 3 and 5 would result in the predominant production of the 3*S*-form of the cyclic ketal (Figure 4), as opposed to the natural 3*R*-form of ATX. However, since the results of a previously published study indicated that **2** with a similar unnatural configuration (3*R* in the case of **2**) exhibited PKC binding and antiproliferative activities,[17] we thought that **4** with a 3S-configuration would exhibit significant biological activity.

2.2 Synthesis of 4

In Scheme 1 is detailed the synthetic route adopted to produce **4**. The synthesis of the known carboxylic acid **7**[23] started from benzyl-(*R*)-(−)-glycidyl ether with vinylmagnesium bromide and CuI, followed by the protection of the hydroxy group as a *tert*-butyldimethylsilyl (TBS) ether, and the oxidative cleavage of the olefin, produced **7**. The synthesis of the carboxylic acid **10** started from dimethyl 3-hydroxyglutarate. Selective reduction of a single carboxy group in dimethyl 3-hydroxyglutarate with borane dimethyl sulfide and $NaBH_4$ furnished diol **8** as a racemic mixture.[24] The subsequent protection of the two hydroxy groups of **8** to form a TBS ether and hydrolysis of the methyl ester group provided **10** as a racemic mixture. Synthesis of alcohol **13** started from (*R*)-(−)-carvone. Epoxidation of (*R*)-(−)-carvone with hydrogen peroxide followed by separation of the minor diastereomer by column chromatography provided epoxide **11** as a single diastereomer.[25] The previously reported reductive alkylation of **11** afforded the known alcohol **12**[25] as a diastereomeric mixture in 88:12 ratio. Following the first esterification step (step j), a column chromatography purification was conducted to result in the separation of the undesired diastereomer. Olefin cross-metathesis[26] between **12** and 4-phenyl-1-butene achieved using second generation Hoveyda–Grubbs catalyst[27] provided a mixture of **13a** and one-carbon-shorter **13b**. Probably, **13b** was generated via cross-metathesis between **12** and 4-phenyl-2-butene formed by catalytic olefin migration[28] of 4-phenyl-1-butene. In neither case was the *Z*-form product obtained. Yamaguchi esterification[29] of **13a**,**b** with **7** produced esters **14a**,**b**; the following deprotection of the TBS group afforded alcohols **15a,b**, respectively. Yamaguchi esterification of **15a**,**b** with the racemic carboxylic acid **10** produced esters **16a**,**b** as diastereomeric mixtures. Macroketalization of **16a**,**b** with trimethylsilyl triflate[30] implementing the previously reported process for the synthesis of **1** and **2**[17] afforded **17a**,**b**, respectively. The observation of nuclear Overhauser effect spectroscopy (NOESY) correlations between H-3 and H-11 and between H-5 and H-11 in **17a,b** (Scheme 1) suggested that, as expected, the 3*S*-forms of cyclic acetals **17a,b** had been obtained and that the 3*R*-forms of **17a,b** had not been produced in the reaction. The possible diastereomer at the acetal position (position 6) was not observed, probably owing to geometrical restriction by the formation of the macrolactone ring. Finally, catalytic hydrogenations of **17a,b** followed by purification by silica-gel column chromatography and reversed-phase high-performance liquid chromatography (HPLC) provided **4** and the one-carbon-shorter **18** via an eight-step LLS with overall yields of 1.8% and 0.4%, respectively. Compounds **4** and **18** were approximately 1.2:1 and 1.3:1 mixtures of epimers at position 12, respectively, but we were unable to separate the diastereomers by normal-phase or reversed-phase HPLC. In summary, we achieved the synthesis of **4** in a smaller number of steps and in higher overall yield than the reported values for 10-Me-aplog-1 (23-step LLS; overall yield, 1.1%),[15] 18-deoxy-aplog-1 (24-step LLS; overall yield, 0.43%),[31] **1** (18-step LLS; overall yield, 0.30%), and **2** (18-step LLS; overall yield, 0.67%).[17]

2.3 Conformational analysis of 4

In Figure 5 are reported the most stable conformations of **4** and 18-deoxy-aplog-1 as they were predicted by the simulated annealing method and density functional theory (DFT) calculations, in which the side-chains were replaced by a methyl group to simplify the calculation. The conformation of the cyclic ketal moiety in 4 was predicted to be *chair–chair*, similarly to the case of 18-deoxy-aplog-1, although in **4** the A ring had a flipped *chair* conformation. The *J* values of H-3 (δ_H = 4.18, tt, *J* = 10.9, 2.8 Hz) and H-8 (δ_H = 4.99, t, *J* = 2.8 Hz) in **4** indicate that these protons are in the axial and equatorial positions, respectively, which is consistent with the predicted most stable conformation of the compound. The predicted conformation was also consistent with the observed nuclear Overhauser effect (NOE) correlations between H-3 and H-11 and between H-5 and H-11 (see Scheme 1). The *J* values of H-26 (δ_H = 2.88, dd, *J* = 18.3, 11.5 Hz; δ_H = 2.61, dd, *J* = 18.3, 3.4 Hz) indicate that the –COOR group at position 26 and the $-CH_2OH$ group at position 27 are in anti conformation to each other, as indicated by the structure drawn in Figure 5. Despite the 3*S*-configuration and flipped chair conformation of the A ring in **4**, the results of DFT calculations

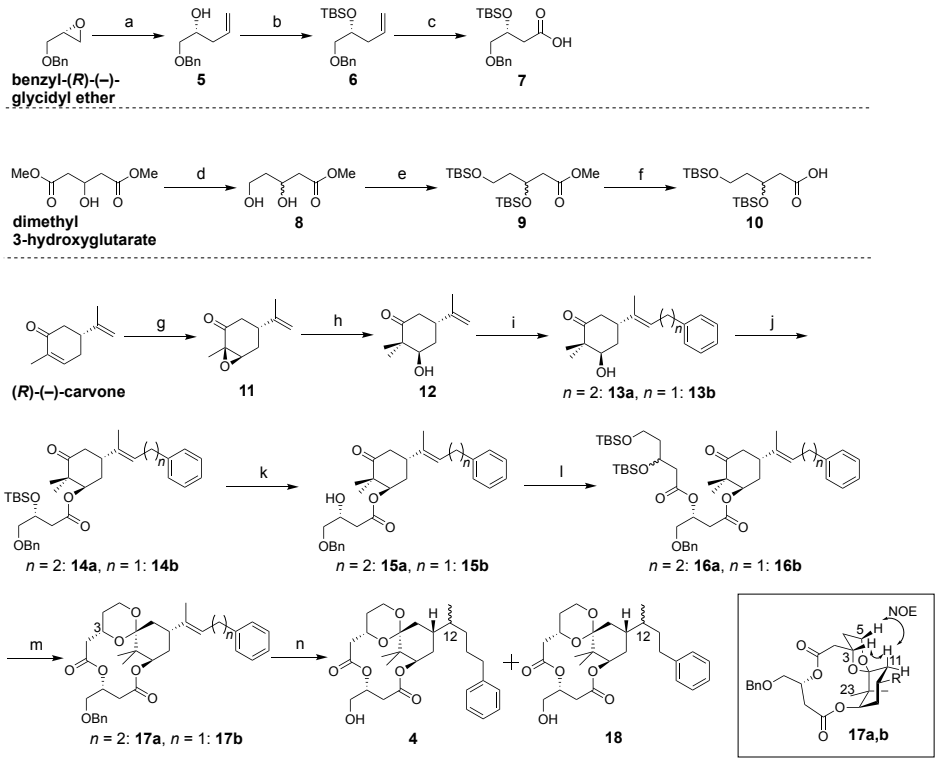

Scheme 1. Synthesis of **4**.

(a) vinylmagnesium bromide, CuI, THF, 88%. (b) *tert*-butyldimethylchloronsilane, imidazole, DMF, 96%. (c) $KMnO_4$, $NaIO_4$, *t*-BuOH, pH 7.0 phosphate buffer, 91%. (d) $BH_3 \cdot SMe_2$, $NaBH_4$, THF, 86%. (e) *tert*-butyldimethylchloronsilane, imidazole, DMF, 92%. (f) LiOH, THF, MeOH, H_2O, 95%. (g) H_2O_2, NaOH aq., MeOH, 89%. (h) Li, NH_3; CH_3I, Et_2O, 64% (dr = 88:12). (i) 4-phenyl-1-butene, 2nd generation Hoveyda–Grubbs catalyst, CH_2Cl_2, 32% (**13a**:**13b** = 4.2:1). (j) 2,4,6-trichlorobenzoyl chloride, Et_3N, CH_2Cl_2; **7**, 4-dimethylaminopyridine, CH_2Cl_2, 75%. (k) HF-pyridine, THF, 70%. (l) 2,4,6-trichlorobenzoyl chloride, Et_3N, toluene; **10**, 4-dimethylaminopyridine, toluene, 95%. (m) trimethylsilyl triflate, CH_2Cl_2, 31% (62% based on (3*S*)-**16**). (n) Pd/C, H_2, MeOH; **4**, 77% (major diastereomer:minor diastereomer = 1.2:1); **18**, 10% (major diastereomer:minor diastereomer = 1:1).

and NMR data suggest that the conformation of the receptor-recognition domain of **4** is similar to that of 18-deoxy-aplog-1.

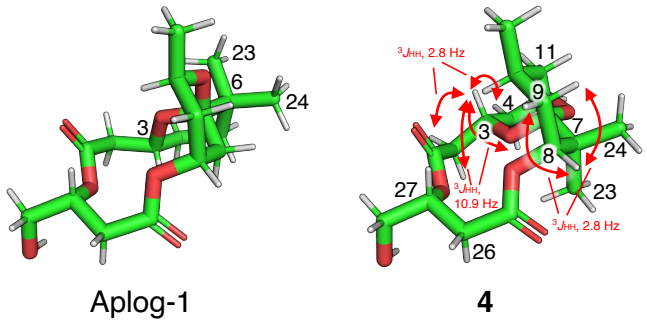

Figure 4: The most stable conformations of Aplog-1 and **4**. Each structure was energetically minimized at the ωB97X-D/6-31G(d,p) level of theory using the Gaussian 16 (Revision C.01) software. The side-chains were replaced by a methyl group to simplify the calculation.

2.4 Binding affinity toward PKC isozymes

Since the antiproliferative activity of aplogs toward cancer cell lines is associated with the activation of PKCα and δ isozymes,[32] we evaluated the binding affinity of **4** and **18** for PKCα and δ implementing the [^{3}H]phorbol 12,13-dibutyrate ([^{3}H]PDBu) displacement assay reported by Sharkey and Blumberg[33] with slight modifications. We used chemically synthesized PKCα-C1A and δ-C1B peptides to conduct the assay,[34] because the PKCα-C1A and δ-C1B domains are the primary binding sites of tumor promoters in PKCα and δ isozymes, respectively. Note that the affinity of the C1 peptides for ligands is comparable to that of the full-length enzymes.[35] In the assay, the binding affinity was expressed as a a binding inhibition constant, K_i, which corresponds with a dissociation constant, K_d. The binding affinity between **4** and α-C1A (K_i, 110 nM) was quite similar to that between 18-deoxy-aplog-1 and α-C1A (K_i, 120 nM). This result is ascribable to the complementation of molecular hydrophobicity and effective shielding of the oxygen atom in the A ring, thus retaining hydrophobicity around the ketal moiety, by the dimethyl group at position 7 (Figure 5). By contrast, the binding affinity between **4** and δ-C1B (K_i, 43 nM) was approximately four times as weak as that between 18-deoxy-aplog-1 and δ-C1B (K_i, 9.8 nM)[31] (Table 1). This result could be due to the unnatural 3*S* configuration of **4**, as it was in the cases for compounds **1** and **2**. The binding affinity of **4** toward the PKC C1 peptides was four to five times weaker than that of **2**. This result be explained by the absence of the 10-methyl group and the phenolic hydroxy groups, which are expected to form a hydrophobic interaction and a hydrogen bond with PKC C1 domains, respectively.[14,31,36] The byproduct **18**, which is characterized by a side chain that is one-carbon-shorter than that of **4**, exhibited a slightly lower binding affinity toward both C1 peptides (K_i for α-C1A, 120 nM; K_i for δ-C1B, 65 nM) than **4** (Table 2). This result is a similar to that previously reported for the analogs of 10-Me-aplog-1 characterized by a side chain that was one-carbon-shorter than 10-Me-aplog-1.[37]

Table 1: K_i values for the inhibition of [^{3}H]PDBu binding by 18-deoxy-Aplog-1, **1**, **2**, **4**, and **18**.

	K_i (nM)				
PKC C1 peptides	18-Deoxy-aplog-1[a]	**1**[b]	**2**[b]	**4**	**18**
α-C1A	120	22	22	110 (10)[c]	120 (10)[c]
δ-C1B	9.8	6.8	13	43 (0)[c]	65 (0)[c]

[a] Data from Ref. 31. [b] Data from Ref. 17. [c] Standard deviation from two separate experiments.

2.5 Antiproliferative activities toward human cancer cell lines

Finally, we evaluated the antiproliferative activities of **4** carrying out the relevant assay using a panel of 39 human cancer cell lines established by Yamori *et al.*[38] In Table 2 are listed the log GI_{50} values obtained for the aplog-sensitive eight cancer cell lines (HBC-4, MDA-MB-231, SF-295, HCC2998, NCI-H460, A549, St-4, and MKN45) and the mean of the log GI_{50} values for these eight cell lines; in this table are also presented the mean graph midpoint (MG-MID) values which are the mean of log GI_{50} values for all 39 cancer cell lines. The GI_{50} (M) value represents the concentration required to inhibit cell growth by 50% compared to the untreated group. PKC activators, including other aplogs, displayed a notable antiproliferative activity toward the eight cell lines listed in Table 2. Similarly, **4** exhibited significant antiproliferative activity (log GI_{50}, < -5) toward seven of the eight cell lines. The mean log GI_{50} value of **4** (-5.48) for the aplog-sensitive cell lines was slightly larger than that of 18-deoxy-aplog-1 (-5.76) and **1** (-5.74), but it was slightly smaller than that measured for **2** (-5.35). The Pearson's correlation coefficient, r, between the log GI_{50} values of 18-deoxy-aplog-1 and **4** toward 39 human cancer cell lines (Supplementary materials) was 0.74, suggesting that 18-deoxy-aplog-1 and **4** share the same mechanism of action. In other words, these results suggest that the activation of PKC isozymes mediates the antiproliferative activity of **4**.

Despite **4** exhibiting inferior PKC-binding ability to **2**, it displayed higher antiproliferative activity than **2**. This discrepancy might be attributable to **4** having higher hydrophobicity (CLogP, 3.9) than **2** (CLogP, 2.1); in fact, the results of a previously published study[39] indicated the optimal log P value of aplogs with respect to their antiproliferative activity to be relatively high (4.0–4.5).

3 Conclusion

In this study, our primary goal was to develop a more synthetically accessible and simplified analog of ATX that exhibited substantial antiproliferative activity. By replacing the positions of the oxygen atom in the B ring, the 6-dimethylmethylene group, and the 8-methylene group within the spiroketal ring of ATX, we designed **4**, which included a cyclic ketal moiety derived from (*R*)-(−)-carvone. As a result, we achieved the synthesis of **4** in a smaller number of steps (eight) and at higher overall yield (1.8%) than 10-Me-aplog-1, 18-deoxy-aplog-1, **1**, and **2**. Despite the considerable difference between the structure of the conformation-controlling unit in **4** and those of other aplogs, the receptor-recognition domain of **4** retained an active conformation similar to those of other aplogs.

Carvone-based analog **4** exhibited antiproliferative activity toward SF-295, NCI-H460, and A549 human cancer cell lines, which was comparable to that of 18-deoxy-aplog-1, even though its affinity for δ-C1B was 4-fold weaker than that of 18-deoxy-aplog-1. These results are indicative of the potential of **4** as a basis for synthesizing a wide variety of ATX analogs that can be obtained with a smaller number of synthetic steps. Such a wide variety of analogs could be a promising chemical library for discovering clinical candidates for PKC-related diseases such as cancer, Alzheimer's disease, and HIV infection.

Table 2: Anti-proliferative activity of 18-deoxy-aplog-1, **1**, **2**, and **4** toward human cancer cell lines

Cancer type	Cell line	log GI_{50} (log M)			
		18-Deoxy-aplog-1[a]	**1**[b]	**2**[b]	**4**
Breast	HBC-4	−6.28	−6.26	−5.88	−4.91
Breast	MDA-MB-231	−5.67	−5.10	−4.95	−5.44
CNS	SF-295	−5.14	−5.50	−4.96	−5.43
Colon	HCC2998	−5.53	−5.56	−5.17	−5.36
Lung	NCI-H460	−5.83	−6.12	−5.69	−5.82
Lung	A549	−5.49	−5.40	−5.20	−5.49
Stomach	St-4	−6.05	−5.96	−5.33	−5.59
Stomach	MKN45	−6.09	−6.00	−5.62	−5.80
mean for the above cell lines		−5.76	−5.74	−5.35	−5.48
MG-MID		−5.09	Not calculated[c]	−4.85	−5.02

[a] Data from Ref. 31. [b] Data from Ref. 17. [c] The MG-MID value for **1** was non-comparable to the values for the other compounds because the highest assay concentration of **1** was −5 (log M), while the others' were −4 (log M).

4 Experimental

4.1 General remarks

The following spectroscopic and analytical instruments were used: ^{1}H and ^{13}C NMR, JEOL JNM-ECZ500 (JEOL, Tokyo, Japan; internal standard, tetramethylsilane (0 ppm) for ^{1}H NMR and $CDCl_3$ (77.0 ppm) for ^{13}C NMR); HPLC, JASCO PU-980 Intelligent HPLC pump with a JASCO PV-970 Intelligent UV/VIS Detector and JASCO PU-4086 Semi-preparative Pump with a JASCO UV-4075 UV/VIS Detector (JASCO, Tokyo, Japan); HR-ESI-TOF-MS, Xevo G2-XS (Waters, Tokyo, Japan) equipped with an ACQUITY UPLC BEH C18 column (Waters, Tokyo, Japan). HPLC was carried out on YMC-Pack ODS-AM AM12S05–1520WT. (YMC, Kyoto, Japan). Wakogel C-300HG (silica gel, FUJIFILM Wako Pure Chemical Corporation, Osaka, Japan) were used for open and flash column chromatography. Preparative thin-layer chromatography was carried out on TLC Silica gel 60 F_{254} (Merck KGaA, Darmstadt, Germany). [^{3}H]PDBu (17.16 Ci/mmol) was custom-synthesized by PerkinElmer Life Science Research Products (Boston, MA, US). The PKC C1 peptides were synthesized as reported previously.[34] All other reagents were purchased from chemical companies and used without further purification. Compound **8** was synthesized as previously described.[24]

4.2 Synthetic procedures

4.2.1 Synthesis of 9

To a solution of **8** (116 mg, 0.784 mmol) in DMF (2.0 mL) were added imidazole (320 mg, 4.81 mmol, 6.1 equiv.) and *tert*-butyldimethylchlorosilane (481 mg, 3.19 mmol, 4.1 equiv) at 0 °C. The reaction mixture was warmed to room temperature and stirred for 23 h. The reaction was quenched with H_2O (24 mL). After the organic layer was separated, the aqueous layer was extracted with Et_2O (24 mL × 3). The combined organic layers were washed with brine, dried over $MgSO_4$, filtered, and concentrated *in vacuo*. The residue was purified by column chromatography (silica gel, hexane:EtOAc = 10:1) to afford **9** (270 mg, 0.718 mmol, 92%). $[\alpha]_D$, +0.0 (*c* 1.2, $CHCl_3$, 24.6 °C). ^{1}H NMR (500 MHz, $CDCl_3$, 0.078 M) δ −0.02 (12H, s), 0.80 (9H, s), 0.82 (9H, s), 1.60–1.71 (2H, m), 2.43 (2H, t, J = 5.2 Hz), 3.59 (3H, s), 3.62 (2H, t,

J = 6.3 Hz), 4.22 (1H, quin, J = 5.7 Hz) ppm; ^{13}C NMR (126 MHz, $CDCl_3$, 0.030 M) δ −5.4 (2C), −4.9, −4.7, 17.9, 18.2, 25.7 (3C), 25.9 (3C), 40.4, 42.8, 51.4, 59.3, 66.8, 172.1 ppm. HR-ESI-MS, m/z 399.2371 ($[M+Na]^+$, calcd. for $C_{18}H_{40}O_4NaSi$, 399.2363).

4.2.2 Synthesis of 10

To a solution of **9** (56.9 mg, 0.151 mmol) in THF (1.0 mL), MeOH (0.50 mL), and H_2O (0.50 mL) was added $LiOH \cdot H_2O$ (25.3 mg, 0.603 mmol, 4.0 equiv) at 0 °C. After the reaction mixture was warmed to room temperature and stirred for 1 h, $LiOH \cdot H_2O$ (7.1 mg, 0.17 mmol, 1.1 equiv.) was added. The reaction mixture was stirred for 1.5 h at same temperature. The reaction was quenched with saturated aq. NH_4Cl (10 mL). After the organic layer was separated, the aqueous layer was washed with EtOAc (10 mL × 3). The organic layer was dried over $MgSO_4$, filtered, and concentrated *in vacuo* to afford **10** (51.9 mg, 0.143 mmol, 95%).

4.2.3 Synthesis of 13a,b

To a solution of **12** (36.6 mg, 0.201 mmol) in CH_2Cl_2 (0.60 mL) was added 2nd generation Hoveyda–Grubbs catalyst (14.5 mg, 23.1 μmol, 12 mol%) in CH_2Cl_2 (0.40 mL) at 40 °C. The flask was fitted with reflux condenser. 4-Phenyl-1-butene (45.1 μL, 0.300 mmol, 1.5 equiv.) in CH_2Cl_2 (0.68 mL) was added dropwise (2.0 μL min^{-1}) and stirred for 6 h at same temperature. After 3 h from the drop started, 2nd generation Hoveyda–Grubbs catalyst (10.0 mg, 16.0 μmol, 7.9 mol%) in CH_2Cl_2 (0.10 mL) was added to the reaction mixture. The reaction mixture was stirred at same temperature for additional 18 h. The resulting solution was filtered with silica gel column, eluting with EtOAc, and concentrated in vacuo. The residue was purified by preparative thin-layer chromatography (PTLC) (silica gel, $CHCl_3$:MeOH = 200:1) to afford **13a,b** (18.2 mg, 29.0 μmol, 32% calculated as **13a**; **13a**:**13b** = 4.2:1 by ^{1}H NMR). $[\alpha]_D$, +37 (c 0.28, $CHCl_3$, 25.1 °C). **13a**: ^{1}H NMR (500 MHz, $CDCl_3$, 0.022 M) δ 1.14 (3H, s), 1.18 (3H, s), 1.54 (3H, s), 1.81–1.86 (1H, m), 2.07 (1H, ddd, J = 14.2, 13.9, 2.2 Hz), 2.27 (1H, ddd, J = 12.3, 4.6, 1.9 Hz), 2.30 (2H, q, J = 8.3 Hz), 2.54 (1H, dd, J = 14.2, 12.6 Hz), 2.64 (2H, t, J = 7.8 Hz), 2.82 (1H, tt, J = 12.3, 4.2 Hz), 3.89 (1H, br.s), 5.26 (1H, t, J = 7.0 Hz), 7.16–7.29 (5H, m) ppm; ^{13}C NMR (126 MHz, $CDCl_3$, 0.038 M) δ 14.0, 20.3, 24.5, 29.8, 33.1, 35.9, 41.0, 42.4, 49.6, 77.7, 123.9, 125.8, 128.2 (2C), 128.5 (2C), 137.2, 142.0, 214.7 ppm. HR-ESI-MS, **13a**: m/z 309.1836 ($[M+Na]^+$, calcd. for $C_{19}H_{26}O_2Na$, 309.1831); **13b**: m/z 295.1671 ($[M+Na]^+$, calcd. for $C_{18}H_{24}O_2Na$, 295.1674).

4.2.4 Synthesis of 14a,b

To a solution of **7** (34.5 mg, 0.108 mmol, 2.1 equiv.) in toluene (170 μL) were added Et_3N (15.1 μL, 0.108 mmol, 2.1 equiv.) and 2,4,6-trichlorobenzoyl chloride (16.8 μL, 0.108 mmol, 2.1 equiv.) at room temperature. After stirred for 1 h at same temperature, **13a,b** (14.9 mg, 52.0 μmol) in toluene (170 μL) and 4-dimethylaminopyridine (13.9 mg, 0.113 mmol, 2.2 equiv.) were added to the reaction mixture. The reaction mixture was warmed to 40 °C and stirred for 46 h. The resulting solution was filtered with silica gel column, eluting with hexane:EtOAc = 1:2, and concentrated *in vacuo*. The residue was purified by column chromatography (silica gel, hexane:EtOAc = 8:1) to afford **14a,b** (23.2 mg, 39.1 μmol, 75% calculated as **14a**). $[\alpha]_D$, +25 (c 0.57, $CHCl_3$, 25.5 °C). **14a**: ^{1}H NMR (500 MHz, $CDCl_3$, 0.0098 M) δ 0.04 (3H, s), 0.05 (3H, s), 0.83 (9H, s), 1.01 (3H, s), 1.20 (3H, s), 1.51 (3H, s), 1.84 (1H, m), 2.04 (1H, ddd, J = 14.6, 12.2, 2.3 Hz), 2.28–2.32 (3H, m), 2.46 (1H, dd, J = 15.7, 7.3 Hz), 2.52 (1H, t, J = 14.2 Hz), 2.58 (1H, dd, J = 18.0, 13.3 Hz), 2.63 (2H, t, J = 7.6 Hz), 2.66 (1H, tt, J = 12.6, 3.7 Hz), 3.33–3.46 (2H, m), 4.29 (1H, m), 4.51 (2H, s), 5.11 (1H, t, J = 2.3 Hz), 5.23 (1H, t, J = 7.4 Hz), 7.13–7.19 (3H, m), 7.25–7.36 (7H, m) ppm; ^{13}C NMR (126 MHz, $CDCl_3$, 0.0098 M) δ −4.97, −4.59, 13.9, 18.0, 20.3, 24.6, 25.8 (3C), 29.8, 30.5, 35.8, 40.1, 41.4, 42.3, 48.1, 68.3, 73.3, 73.9, 78.9, 124.0, 125.8, 127.6, 127.6 (2C), 128.2 (2C), 128.3 (2C),

128.4 (2C), 136.6, 138.1, 141.9, 170.6, 213.3 ppm. HR-ESI-MS, **14a**: *m/z* 615.3483 ([M+Na]$^+$, calcd. for $C_{36}H_{52}O_5NaSi$, 615.3482); **14b**: *m/z* 601.3332 ([M+Na]$^+$, calcd. for $C_{35}H_{50}O_5NaSi$, 601.3326).

4.2.5 Synthesis of 15a,b

To a solution of **14a,b** (22.2 mg, 37.4 μmol) in THF (1.3 mL) was added HF-pyridine (70% HF, 280 μL) at 0 °C. After the reaction mixture was warmed to room temperature and stirred for 22 h, the reaction was quenched with dropwise addition of saturated aq. $NaHCO_3$ (6.0 mL). After the organic layer was separated, the aqueous layer was washed with EtOAc (6.0 mL × 3). The organic layer was dried over $MgSO_4$, filtered, and concentrated *in vacuo*. The residue was purified by column chromatography (silica gel, hexane:EtOAc = 3:1) to afford **15a,b** (12.5 mg, 26.1 μmol, 70% calculated as **15a**). $[\alpha]_D$, +23 (*c* 0.60, $CHCl_3$, 17.0 °C). **15a**: ^{1}H NMR (500 MHz, $CDCl_3$, 0.0065 M) δ 1.04 (3H, s), 1.22 (3H, s), 1.51 (3H, s), 1.87 (1H, m), 2.05 (1H, td, *J* = 12.6, 2.9 Hz), 2.28–2.32 (3H, m), 2.52 (2H, m), 2.63 (2H, t, *J* = 8.0 Hz), 2.67–2.76 (1H, m), 2.80 (1H, br.s), 3.34 (1H, dd, *J* = 9.4, 4.7 Hz), 3.49 (1H, dd, *J* = 9.6, 4.3 Hz), 4.22 (1H, m), 4.54 (2H, s), 5.13 (1H, dd, *J* = 3.7, 2.6 Hz), 5.23 (1H, t, *J* = 6.9 Hz), 7.14–7.19 (3H, m), 7.25–7.37 (7H, m) ppm; ^{13}C NMR (126 MHz, $CDCl_3$, 0.0065 M) δ 13.9, 20.3, 24.6, 29.8, 30.5, 35.8, 38.4, 41.5, 42.3, 48.0, 67.2, 73.1, 73.5, 79.5, 124.2, 125.8, 127.8 (2C), 127.9 (2C), 128.3 (2C), 128.5 (3C), 136.6, 137.7, 141.9, 171.1, 213.3 ppm. HR-ESI-MS, **15a**: *m/z* 501.2627 ([M+Na]$^+$, calcd. for $C_{30}H_{38}O_5Na$, 501.2617); **15b**: *m/z* 487.2459 ([M+Na]$^+$, calcd. for $C_{29}H_{36}O_5Na$, 487.2461).

4.2.6 Synthesis of 16a,b

To a solution of **10** (40.4 mg, 111 μmol, 2.1 equiv.) in toluene (210 μL) were added Et_3N (15.5 μL, 0.111 mmol, 2.1 equiv.) and 2,4,6-trichloreobenzoyl chloride (17.3 μL, 111 μmol, 2.1 equiv.) at room temperature. After stirred at same temperature for 1 h, the reaction mixture was added **15a,b** (25.3 mg, 52.9 μmol) in toluene (210 μL) and 4-dimethylaminopyridine (13.6 mg, 0.111 μmol, 2.1 equiv.). The reaction mixture was stirred for 24 h at same temperature. The resulting solution was filtered with silica gel column, eluting with hexane:EtOAc = 1:2, and concentrated *in vacuo*. The residue was purified by PTLC (silica gel, benzene:EtOAc = 10:1) to afford **16a,b** (41.4 mg, 50.2 μmol, 95% calculated as **16a**). $[\alpha]_D$, +11 (*c* 0.94, $CHCl_3$, 28.9 °C). **16a**: ^{1}H NMR (500 MHz, $CDCl_3$, 0.0047 M) δ 0.04 (9H, s), 0.06 (3H, s), 0.84 (6H, s), 0.85 (3H, s), 0.87 (9H, s), 1.01 (3H, s), 1.20 (3H, s), 1.52 (3H, s), 1.69–1.72 (2H, m), 1.83 (1H, dd, *J* = 14.4, 4.2 Hz), 2.06 (1H, quintet, *J* = 14.3 Hz), 2.31 (2H, m), 2.48 (2H, dd, *J* = 5.7, 3.4 Hz), 2.50–2.60 (2H, m), 2.64 (2H, t, *J* = 8.0 Hz), 2.66–2.75 (3H, m), 3.53 (1H, m), 3.61 (1H, dd, *J* = 10.3, 4.6 Hz), 3.66 (2H, t, *J* = 5.2 Hz), 4.25 (1H, m), 4.45–4.55 (2H, m), 5.10 (1H, t, *J* = 2.9 Hz), 5.24 (1H, t, *J* = 6.9 Hz), 5.32 (1H, m), 7.14–7.20 (3H, m), 7.25–7.35 (7H, m) ppm; ^{13}C NMR (126 MHz, $CDCl_3$, 0.0047 M) δ −5.3 (2C), −4.7 (2C), 14.0, 18.0, 18.2, 20.2, 24.5, 25.8 (3C), 26.0 (3C), 29.8, 30.5, 35.8, 40.1, 40.2, 41.3, 42.3, 42.7, 48.0, 59.4, 66.4, 68.9, 70.0, 73.3, 79.2, 124.1, 125.8, 127.7, 127.8 (2C), 128.2 (2C), 128.3 (2C), 128.4 (2C), 136.6, 137.7, 141.9, 169.3, 170.7, 213.0 ppm. HR-ESI-MS, **16a**: *m/z* 845.4811 ([M+Na]$^+$, calcd. for $C_{47}H_{74}O_8NaSi_2$, 845.4820); **16b**: *m/z* 831.4655 ([M+Na]$^+$, calcd. for $C_{46}H_{72}O_8NaSi_2$, 831.4664).

4.2.7 Synthesis of 17a,b

To a solution of **17a,b** (41.4 mg, 50.2 μmol) in CH_2Cl_2 (2.6 mL) was added TMSOTf (9.0 μL, 50 μmol, 1.0 eq.) at −40 °C. The reaction mixture was stirred for 8 h at same temperature. After 3 h and 6 h from starting the reaction, TMSOTf (4.5 μL, 25 μmol, 0.5 eq.) was added to the reaction mixture. The reaction was quenched with pyridine (59 μL) and concentrated *in vacuo*. The residue was purified by column chromatography (silica gel, hexane:EtOAc = 5:1) and PTLC (silica gel, hexane:EtOAc = 3:1) to afford **17a,b** (9.0 mg, 16 μmol, 31% calculated as **17a**). $[\alpha]_D$ +50 (*c* 0.94, $CHCl_3$, 23.0 °C). **17a**: ^{1}H NMR (500

MHz, $CDCl_3$, 0.039 M) δ 0.99 (3H, s), 0.99 (3H, s), 1.20–1.40 (1H, m), 1.42–1.54 (1H, m), 1.50 (3H, s), 1.57–1.63 (2H, m), 1.68–1.81 (1H, m), 2.27–2.47 (6H, m), 2.65 (2H, t, *J* = 8.6 Hz), 2.70 (1H, d, *J* = 17.8 Hz), 2.93 (1H, dd, *J* = 18.3, 10.9 Hz), 3.47 (1H, dd, *J* = 9.9, 6.0 Hz), 3.56 (1H, dd, *J* = 9.9, 6.0 Hz), 3.80 (1H, m), 4.00 (1H, td, *J* = 12.0, 2.3 Hz), 4.26 (1H, tt, *J* = 10.9, 2.9 Hz), 4.55 (2H, ABq, *J* = 11.5 Hz), 5.00 (1H, t, *J* = 2.9 Hz), 5.27 (1H, t, *J* = 6.9 Hz), 5.35 (1H, m), 7.16–7.19 (3H, m), 7.25–7.36 (7H, m) ppm; ^{13}C NMR (126 MHz, $CDCl_3$, 0.039 M) δ 14.1, 18.8, 21.7, 27.8, 30.0, 30.7, 31.5, 36.0, 36.7, 37.3, 42.5, 42.6, 58.9, 66.9, 68.8, 70.7, 73.4, 78.0, 100.2, 123.2, 125.7, 127.7, 127.8 (2C), 128.4 (2C), 128.4 (2C), 128.5 (2C), 137.6, 138.4, 142.4, 169.6, 172.2 ppm. HR-ESI-MS, **17a**: *m/z* 599.2985 ($[M+Na]^+$, calcd. for $C_{35}H_{44}O_7Na$, 599.2991); **17b**: *m/z* 585.2834 ($[M+Na]^+$, calcd. for $C_{34}H_{42}O_7Na$, 585.2829).

4.2.8 Synthesis of 4 and 18

To a solution of **17a,b** (3.7 mg, 6.4 μmol) in MeOH (0.80 mL) was added 10% Pd/C (2.7 mg) at room temperature. The mixture was stirred under H_2 atmosphere for 2 h at same temperature. The resulting mixture was filtered and concentrated *in vacuo*. The residue was purified by column chromatography (silica gel, hexane:EtOAc = 2:1) and HPLC (column, YMC-Pack ODS-AM AM12S05–1520WT; solvent, MeOH:H_2O = 7:1; flow rate 8.0 mL min^{-1}; retention time, 10.1 min for **18** and 11.9 min for **4**) to afford **18** (0.3 mg, 0.6 μmol, 10%) and **4** (2.4 mg, 4.9 μmol, 77%).

Compound 4 (major diastereomer:minor diastereomer = 1.2:1); $[\alpha]_D$, +47 (*c* 0.43, $CHCl_3$, 26.2 °C). **Major diastereomer**: ^1H NMR (500 MHz, $CDCl_3$, 0.012 M) δ 0.87 (3H, d, *J* = 6.9 Hz, H-22), 0.97 (3H, s, H-23 or H-24), 0.98 (3H, s, H-23 or H-24), 1.10 (1H, t, *J* = 13.2 Hz, H-11 axial), 1.19–1.28 (1H, m, H-13a), 1.32–1.52 (4H, m, H-4a, H-9, H-12, H-13b), 1.53–1.78 (5H, m, H-4b, H-9, H-10, H-14), 1.86 (1H, br s, 28-OH) 2.34–2.48 (3H, m, H-2, H-11 equatorial), 2.55–2.67 (2H, m, H-15), 2.61 (1H, dd, *J* = 18.3, 3.4 Hz, H-26a), 2.88 (1H, dd, *J* = 18.3, 11.5 Hz, H-26b), 3.55–3.70 (2H, m, H-28), 3.79 (1H, dd, *J* = 12.0, 4.0 Hz, H-5 equatorial), 3.98 (1H, td, *J* = 12.0, 2.9 Hz, H-5 axial), 4.12 (1H, tt, *J* = 10.9, 2.9 Hz, H-3), 4.99 (1H, t, *J* = 2.7 Hz, H-8), 5.23 (1H, dt, *J* = 10.9, 5.0 Hz, H-27), 7.17 (1H, t, *J* = 6.9 Hz, H-19), 7.23 (2H, d, *J* = 7.4 Hz, H-17, H-21), 7.28 (2H, t, *J* = 8.0 Hz, H-18, H-20) ppm; ^{13}C NMR (126 MHz, $CDCl_3$, 0.012 M) δ 15.9 (C-22), 18.8 (C-23 or C-24), 21.7(C-23 or C-24), 24.4 (C-11), 28.1 (C-4), 29.0 (C-14), 30.8 (C-10), 32.6 (C-9), 33.8 (C-13), 36.2 (C-15), 36.3 (C-12), 36.4 (C-26), 42.6 (C-2), 42.8 (C-7), 58.7 (C-5), 64.6 (C-28), 66.8 (C-3), 71.1 (C-27), 78.4 (C-8), 100.4 (C-6), 125.6 (C-19), 128.2 (2C, C-17, C-21 or C-18, C-20), 128.4 (2C, C-17, C-21 or C-18, C-20), 142.9 (C-16), 169.3 (C-25), 173.0 (C-1) ppm. **Minor diastereomer**: ^1H NMR (500 MHz, $CDCl_3$, 0.010 M) δ 0.86 (3H, d, *J* = 6.3 Hz, H-22), 0.97 (3H, s, H-23 or H-24), 0.98 (3H, s, H-23 or H-24), 1.20 (1H, t, *J* = 13.2 Hz, H-11 axial), 1.19–1.28 (1H, m, H-13a), 1.32–1.52 (4H, m, H-4a, H-9, H-12, H-13b), 1.53–1.78 (5H, m, H-4a, H-9, H-10, H-14), 1.86 (1H, br s, 28-OH), 2.34–2.48 (3H, m, H-2, H-11 equatorial), 2.55–2.67 (2H, m, H-15), 2.61 (1H, dd, *J* = 18.3, 3.4 Hz, H-26), 2.85 (1H, dd, *J* = 18.3, 11.5 Hz, H-26), 3.55–3.70 (2H, m, H-28), 3.78 (1H, dd, *J* = 12.0, 4.0 Hz, H-5 equatorial), 3.97 (1H, td, *J* = 12.0, 2.9 Hz, H-5 axial), 4.19 (1H, tt, *J* = 10.9, 2.8 Hz, H-3), 4.99 (1H, t, *J* = 2.7 Hz, H-8), 5.16 (1H, dt, *J* = 10.9, 5.0 Hz, H-27), 7.17 (1H, t, *J* = 6.9 Hz, H-19), 7.23 (2H, d, *J* = 7.4 Hz, H-17, H-21), 7.28 (2H, t, *J* = 8.0 Hz, H-18, H-20) ppm; ^{13}C NMR (126 MHz, $CDCl_3$, 0.010 M) δ 16.0 (C-22), 18.8 (C-23 or C-24), 21.7 (C-23 or C-24), 26.5 (C-11), 28.1 (C-4), 29.0 (C-14), 30.8 (C-10), 32.0 (C-9), 33.6 (C-13), 36.2 (C-15), 36.3 (C-12), 36.5 (C-26), 42.6 (C-2), 42.8 (C-7), 58.7 (C-5), 64.7 (C-28), 66.9 (C-3), 71.0 (C-27), 78.3 (C-8), 100.4 (C-6), 125.6 (C-19), 128.2 (2C, C-17, C-21 or C-18, C-20), 128.4 (2C, C-17, C-21 or C-18, C-20), 142.9 (C-16), 169.3 (C-25), 173.0 (C-1) ppm. HR-ESI-MS, *m/z* 511.2670 ($[M+Na]^+$, calcd. for $C_{28}H_{40}O_7Na$, 511.2682).

Compound 18 (major diastereomer:minor diastereomer = 1.3:1); $[\alpha]_D$, +30 (*c* 0.11, $CHCl_3$, 26.6 °C). **Major diastereomer**: ^1H NMR (500 MHz, $CDCl_3$, 3.3 mM) δ 0.94 (3H, d, *J* = 6.3 Hz), 0.97 (3H, s), 0.98 (3H, s), 1.13–1.30 (1H, m), 1.35–1.52 (4H, m), 1.55–1.91 (4H, m), 2.38–2.49 (3H, m), 2.53–2.64 (1H, m), 2.60 (1H, dd, *J* = 18.3, 2.9 Hz), 2.67–2.76 (1H, m), 2.90 (1H, dd, *J* = 18.3, 11.5 Hz), 3.62–3.72 (2H, m), 3.82 (1H, ddd, *J* = 12.0, 5.2, 2.3 Hz), 3.99 (1H, td, *J* = 12.0, 2.9 Hz), 4.23 (1H, tt, *J* = 10.3, 2.9 Hz),

5.01 (1H, t, J = 2.9 Hz), 5.28 (1H, dt, J = 10.9, 5.7 Hz), 7.17–7.31 (5H, m) ppm; ^{13}C NMR (126 MHz, $CDCl_3$, 3.3 mM) δ 15.8, 18.9, 21.7, 24.3, 28.6, 30.8, 32.8, 33.7, 35.7, 36.3, 36.3, 42.6, 42.8, 58.8, 64.8, 66.8, 71.1, 78.3, 100.4, 125.7, 128.3 (2C), 128.5 (2C), 143.0, 169.3, 176.0 ppm. **Minor diastereomer**: ^{1}H NMR (500 MHz, $CDCl_3$, 2.5 mM) δ 0.95 (3H, d, J = 6.3 Hz), 0.97 (3H, s), 0.98 (3H, s), 1.13–1.30 (1H, m), 1.35–1.52 (4H, m), 1.55–1.91 (4H, m), 2.38–2.49 (3H, m), 2.53–2.64 (1H, m), 2.60 (1H, dd, J = 18.3, 2.9 Hz), 2.67–2.76 (1H, m), 2.89 (1H, dd, J = 18.3, 11.5 Hz), 3.62–3.72 (2H, m), 3.79 (1H, ddd, J = 12.0, 5.2, 2.3 Hz) 4.02 (1H, td, J = 12.0, 2.9 Hz), 4.25 (1H, tt, J = 10.3, 2.9 Hz), 5.01 (1H, t, J = 2.9 Hz), 5.26 (1H, dt, J = 10.9, 5.7 Hz), 7.17–7.31 (5H, m) ppm; ^{13}C NMR (126 MHz, $CDCl_3$, 2.5 mM) δ 16.1, 18.9, 21.7, 26.2, 28.6, 30.4, 32.6, 33.7, 35.7, 36.2, 36.4, 42.6, 42.8, 58.8, 64.7, 66.9, 71.1, 78.3, 100.4, 125.7, 128.3 (2C), 128.4 (2C), 143.0, 169.3, 176.1 ppm. HR-ESI-MS, m/z 497.2536 ($[M+Na]^+$, calcd. for $C_{27}H_{38}O_7Na$, 497.2515).

4.3 Conformational search and DFT calculation

The three-dimensional structure of **4** was built using the Avogadro (version 1.2.0) software. Simulated annealing was carried out using the GROMACS program (version 2021.3) with a general AMBER force field 2 (GAFF2) and the AM1-BCC charge calculated by the Antechamber package in the AmberTools21 package. The side chain was replaced by a methyl group to simplify the calculation. All bonds were constrained using the LINCS algorithm. The time step was set to 1 fs. The annealing temperature was initially set to 1,500 K and the temperature was kept constant for 2 ps. The temperature was linearly dropped to 100 K over 1 ps and then to 0 K over 1 ps, and kept at the same temperature for 1 ps. This 5-ps cycle was repeated 1,000 times to give a conformer library, from which the reasonable conformer consistent with the NMR data was selected. The selected conformer was optimized at the M06-2X/aug-cc-pVTZ level of theory using the Gaussian16 program.

4.4 Inhibition of specific binding of [^{3}H]PDBu to PKC C1 peptides

The binding of [^{3}H]PDBu to the PKCα-C1A and δ-C1B peptides was evaluated by the procedure of Sharkey and Blumberg,[33] with modification as reported previously,[35] using 50 mM Tris-maleate buffer (pH 7.4 at 4 °C), 40 nM PKCα-C1A or 13.8 nM PKCδ-C1B peptides, 20 nM [^{3}H]PDBu (17.16 Ci/mmol), 50 μg/mL 1,2-dioleoyl-*sn*-glycero-3-phospho-L-serine, 3 mg/mL bovine γ-globulin, and various concentrations of **4** and **18**. Binding affinity was determined based on the concentration required to cause 50% inhibition of specific binding of [^{3}H]PDBu (IC_{50}), which was calculated by logit procedure. The inhibition constant (K_i) was calculated by the Goldstein-Barrett equation as described previously.[40]

4.5 Measurements of cell growth inhibition

A panel of 39 human cancer cell lines established by Yamori *et al.*[38] was employed. The cells were seeded on 96-well plates in Roswell Park Memorial Institute 1640 (RPMI-1640) medium supplemented with 5% fetal bovine serum and allowed to attach overnight. After the cell was incubated with 4 for 48 h, cell growth was estimated by sulforhodamine B assay. The 50% growth inhibition (GI_{50}) parameter was calculated as reported previously.[38] Absorbance for the control well (C) and the test well (T) was measured at 525 nm along with that for the test well at time 0 (T_0). Cell growth inhibition (% growth) by each concentration of **4** (10^{-8}, 10^{-7}, 10^{-6}, 10^{-5} and 10^{-4}) was calculated as $100[(T - T_0)/(C - T_0)]$ using the average of duplicate points. By processing of these values, GI_{50} value, defined as $100[(T - T_0)/(C - T_0)] = 50$, was determined.

Acknowledgements

The authors thank the Molecular Profiling Committee, Grant-in-Aid for Scientific Research on Innovative Areas "Advanced Animal Model Support (AdAMS)" from the Ministry of Education, Culture, Sports, Science and Technology, Japan (JSPS KAKENHI Grant Number JP 16H06276).

The DFT calculation was performed using Research Center for Computational Science, Okazaki, Japan (Project: 21-IMS-C185).

Supplementary material

Supplementary material to this article can be found online at `https://doi.org/10.1093/bbb/zbac084`.

Data availability

The data underlying this article are available in the article and in its online supplementary material.

Author's Contribution

Y.S. synthesized the compounds, evaluated them, and wrote the paper. K.M. and M.K. synthesized the compounds. R.C.Y. designed the work and wrote the paper. Y.K. designed the target compounds, planed their synthetic route, and wrote the paper. Y.H. provided the direction for the synthetic route and wrote the paper. K.I. supervised the work and wrote the paper.

Funding

This work was supported by JSPS KAKENHI Grant No.17H06405 (to K.I. and R.C.Y.).

Disclosure statement

The authors declare no conflict of interest associated with this manuscript.

References

[1] Yasutomi Nishizuka. The role of protein kinase C in cell surface signal transduction and tumour promotion. *Nature*, 308:693–698, 1984.

[2] Yasutomi Nishizuka. Protein kinase C and lipid signaling for sustained cellular responses. *The FASEB Journal*, 9(7):484–496, 1995.

[3] Corina E. Antal, Andrew M. Hudson, Emily Kang, Ciro Zanca, Christopher Wirth, Natalie L. Stephenson, Eleanor W. Trotter, Lisa L. Gallegos, Crispin J. Miller, Frank B. Furnari, Tony Hunter, John Brognard, and Alexandra C. Newton. Cancer-associated protein kinase C mutations reveal kinase's role as tumor suppressor. *Cell*, 160(3):489–502, 2015.

[4] Alexandra C. Newton. Protein kinase C as a tumor suppressor. *Seminar in Cancer Biology*, 48:18–26, 2018.

[5] Monique Castagna, Yoshimi Takai, Kozo Kaibuchi, Kimihiko Sano, Ushio Kikkawa, and Yasutomi Nishizuka. Direct activation of calcium-activated, phospholipid-dependent protein kinase by tumor-promoting phorbol esters. *Journal of Biological Chemistry*, 257(13):7847–7851, 1982.

[6] Hirota Fujiki and Takashi Sugimura. New Classes of Tumor Promoters: Teleocidin, Aplysiatoxin, and Palytoxin. *Advances in Cancer Research*, 49:223–264, 1987.

[7] Y. Ono, T. Fujii, K. Igarashi, T. Kuno, C. Tanaka, U. Kikkawa, and Y. Nishizuka. Phorbol ester binding to protein kinase C requires a cysteine-rich zinc-finger-like sequence. *Proceedings of the National Academy of Sciences of the United States of America*, 86(13):4868–4871, 1989.

[8] James H. Hurley, Alexandra C. Newton, Peter J. Parker, Peter M. Blumberg, and Yasutomi Nishizuka. Taxonomy and function of C1 protein kinase C homology domains. *Protein Science*, 6(2):477–480, 1997.

[9] Alexandra C. Newton. Protein kinase C: Structural and spatial regulation by phosphorylation, cofactors, and macromolecular interactions. *Chemical Reviews*, 101(8):2353–2364, 2001.

[10] Roger Mutter and Martin Wills. Chemistry and clinical biology of the bryostatins. *Bioorganic and Medicinal Chemistry*, 8(8):1841–1860, 2000.

[11] Peter Kollár, Josef Rajchard, Zuzana Balounová, and Jiří Pazourek. Marine natural products: Bryostatins in preclinical and clinical studies. *Pharmaceutical Biology*, 52(2):237–242, 2014.

[12] Yu Nakagawa, Ryo C. Yanagita, Naoko Hamada, Akira Murakami, Hideyuki Takahashi, Naoaki Saito, Hiroshi Nagai, and Kazuhiro Irie. A simple analogue of tumor-promoting aplysiatoxin is an antineoplastic agent rather than a tumor promoter: Development of a synthetically accessible protein kinase C activator with bryostatin-like activity. *Journal of the American Chemical Society*, 131(22):7573–7579, 2009.

[13] Kazuhiro Irie, Masayuki Kikumori, Hiroaki Kamachi, Keisuke Tanaka, Akira Murakami, Ryo C. Yanagita, Harukuni Tokuda, Nobutaka Suzuki, Hiroshi Nagai, Kiyotake Suenaga, and Yu Nakagawa. Synthesis and structure-activity studies of simplified analogues of aplysiatoxin with antiproliferative activity like bryostatin-1. *Pure and Applied Chemistry*, 84(6):1341–1351, 2012.

[14] Masayuki Kikumori, Ryo C. Yanagita, Harukuni Tokuda, Nobutaka Suzuki, Hiroshi Nagai, Kiyotake Suenaga, and Kazuhiro Irie. Structure-activity studies on the spiroketal moiety of a simplified analogue of debromoaplysiatoxin with antiproliferative activity. *Journal of Medicinal Chemistry*, 55(11):5614–5626, 2012.

[15] Masayuki Kikumori, Ryo C. Yanagita, and Kazuhiro Irie. Improved and large-scale synthesis of 10-methyl-aplog-1, a potential lead for an anticancer drug. *Tetrahedron*, 70(52):9776–9782, 2014.

[16] Fu Min Zhang, Shu Yu Zhang, and Yong Qiang Tu. Recent progress in the isolation, bioactivity, biosynthesis, and total synthesis of natural spiroketals. *Natural Product Reports*, 35(1):75–104, 2018.

[17] Koutaro Hayakawa, Yusuke Hanaki, Harukuni Tokuda, Ryo C. Yanagita, Yu Nakagawa, Mutsumi Okamura, Shingo Dan, and Kazuhiro Irie. Synthesis and Biological Activities of Acetal Analogs at Position 3 of 10-Methyl-Aplog-1, a Potential Anti-Cancer Lead Derived from Debromoaplysiatoxin. *Heterocycles*, 97(1):478–492, 2018.

[18] Robert R. Rando and Yoshito Kishi. Structural Basis of Protein Kinase C Activation by Diacylglycerols and Tumor Promoters. *Biochemistry*, 31(8):2211–2218, 1992.

[19] Yoshito Kishi and Robert R. Rando. Structural Basis of Protein Kinase C Activation by Tumor Promoters. *Accounts of Chemical Research*, 31(4):163–172, apr 1998.

[20] Henner Knust and Reinhard W. Hoffmann. Synthesis and conformational analysis of macrocyclic dilactones mimicking the pharmacophore of aplysiatoxin. *Helvetica Chimica Acta*, 86(6):1871–1893, 2003.

[21] Yoshiki Ashida, Ryo C. Yanagita, Chise Takahashi, Yasuhiro Kawanami, and Kazuhiro Irie. Binding mode prediction of aplysiatoxin, a potent agonist of protein kinase C, through molecular simulation and structure–activity study on simplified analogs of the receptor-recognition domain. *Bioorganic and Medicinal Chemistry*, 24(18):4218–4227, 2016.

[22] Masayuki Kikumori, Ryo C. Yanagita, Harukuni Tokuda, Kiyotake Suenaga, Hiroshi Nagai, and Kazuhiro Irie. Structural optimization of 10-methyl-aplog-1, a simplified analog of debromoaplysiatoxin, as an anticancer lead. *Bioscience, Biotechnology, and Biochemistry*, 80(2):221–231, 2016.

[23] Robert D. Walkup and Raymond T. Cunningham. Studies on the syntheses of the aplysiatoxins: Synthesis of a selectively-protected form of the C_{27}–C_{30} (dihydroxybutanoate) moiety of oscillatoxin A. *Tetrahedron Letters*, 28(35):4019–4022, jan 1987.

[24] Valéria B. Riatto, Maria N.M. Carneiro, Venília B. Carvalho, and Mauricio M. Victor. Efficient synthesis of 1,3,5-oxygenated synthons from dimethyl 3-oxoglutarate: First use of borane-dimethyl sulfide complex as a regioselective reducing agent of 3-oxygenated glutarate derivatives. *Journal of the Brazilian Chemical Society*, 22(1):172–175, 2011.

[25] Shital K. Chattopadhyay, Swastik Karmakar, and Kaushik Sarkar. Short New Route to the Chiral Spiro-Tetrahydrofuran Subunit Common to Some Terpenoids. *Synthetic Communications*, 35(16):2125–2132, aug 2005.

[26] Tina M. Trnka and Robert H. Grubbs. The development of L_2X_2RU=CHR olefin metathesis catalysts: An organometallic success story. *Accounts of Chemical Research*, 34(1):18–29, 2001.

[27] Arnab K. Chatterjee, Tae Lim Choi, Daniel P. Sanders, and Robert H. Grubbs. A general model for selectivity in olefin cross metathesis. *Journal of the American Chemical Society*, 125(37):11360–11370, 2003.

[28] Damien Bourgeois, Ange Pancrazi, Steven P. Nolan, and Joëlle Prunet. The $Cl_2(PCy_3)$(IMes)Ru(=CHPh) catalyst: Olefin metathesis versus olefin isomerization. *Journal of Organometalic Chemistry*, 643-644:247–252, 2002.

[29] Junji Inanaga, Kuniko Hirata, Hiroko Saeki, Tsutomu Katsuki, and Masaru Yamaguchi. A Rapid Esterification by Means of Mixed Anhydride and Its Application to Large-ring Lactonization. *Bulletin of the Chemical Society of Japan*, 52(7):1989–1993, 1979.

[30] R. Noyori, S. Murata, and M. Suzuki. Trimethysilyl triflate in organic synthesis. *Tetrahedron*, 37(23):3899–3910, 1981.

[31] Ryo C. Yanagita, Hiroaki Kamachi, Keisuke Tanaka, Akira Murakami, Yu Nakagawa, Harukuni Tokuda, Hiroshi Nagai, and Kazuhiro Irie. Role of the phenolic hydroxyl group in the biological activities of simplified analogue of aplysiatoxin with antiproliferative activity. *Bioorganic and Medicinal Chemistry Letters*, 20(20):6064–6066, 2010.

[32] Yusuke Hanaki, Yuki Shikata, Masayuki Kikumori, Natsuki Hotta, Masaya Imoto, and Kazuhiro Irie. Identification of protein kinase C isozymes involved in the anti-proliferative and pro-apoptotic activities of 10-Methyl-aplog-1, a simplified analog of debromoaplysiatoxin, in several cancer cell lines. *Biochemical and Biophysical Research Communications*, 495(1):438–445, 2018.

[33] Nancy A. Sharkey and Peter M. Blumberg. Highly lipophilic phorbol esters as inhibitors of specific [^{3}H]phorbol 12,13-dibutyrate binding. *Cancer Research*, 45:19–24, 1985.

[34] Kazuhiro Irie, Kentaro Oie, Akifumi Nakahara, Yoshiaki Yanai, Hajime Ohigashi, Paul A. Wender, Hiroyuki Fukuda, Hiroaki Konishi, and Ushio Kikkawa. Molecular basis for protein kinase C isozyme-selective binding: The synthesis, folding, and phorbol ester binding of the cysteine-rich domains of all protein kinase C isozymes. *Journal of the American Chemical Society*, 120(36):9159–9167, 1998.

[35] Mayumi Shindo, Kazuhiro Irie, Akifumi Nakahara, Hajime Ohigashi, Hiroaki Konishi, Ushio Kikkawa, Hiroyuki Fukuda, and Paul A. Wender. Toward the identification of selective modulators of protein kinase C (PKC) isozymes: Establishment of a binding assay for PKC isozymes using synthetic C1 peptide receptors and identification of the critical residues involved in the phorbol ester binding. *Bioorganic and Medicinal Chemistry*, 9(8):2073–2081, 2001.

[36] Yusuke Hanaki, Masayuki Kikumori, Harukuni Tokuda, Mutsumi Okamura, Shingo Dan, Naoko Adachi, Naoaki Saito, Ryo C. Yanagita, and Kazuhiro Irie. Loss of the Phenolic Hydroxyl Group and Aromaticity from the Side Chain of Anti-Proliferative 10-Methyl-aplog-1, a Simplified Analog of Aplysiatoxin, Enhances Its Tumor-Promoting and Proinflammatory Activities. *Molecules*, 22(4):631, apr 2017.

[37] Atsuko Gonda, Koji Takada, Ryo C Yanagita, Shingo Dan, and Kazuhiro Irie. Effects of side chain length of 10-methyl-aplog-1, a simplified analog of debromoaplysiatoxin, on PKC binding, anti-proliferative, and pro-inflammatory activities. *Bioscience, Biotechnology, and Biochemistry*, 85(1):168–180, 2021.

[38] Takao Yamori, Akio Matsunaga, Shigeo Sato, Kanami Yamazaki, Akiko Komi, Kazuhiro Ishizu, Izumi Mita, Hajime Edatsugi, Yasuhiro Matsuba, Kimiko Takezawa, Osamu Nakanishi, Hiroshi Kohno, Yuki Nakajima, Hironori Komatsu, Toshio Andoh, and Takashi Tsuruo. Potent antitumor activity of MS-247, a novel DNA minor groove binder, evaluated by an in vitro and in vivo human cancer cell line panel. *Cancer Research*, 59(16):4042–4049, 1999.

[39] Hiroaki Kamachi, Keisuke Tanaka, Ryo C. Yanagita, Akira Murakami, Kazuma Murakami, Harukuni Tokuda, Nobutaka Suzuki, Yu Nakagawa, and Kazuhiro Irie. Structure-activity studies on the side chain of a simplified analog of aplysiatoxin (aplog-1) with anti-proliferative activity. *Bioorganic and Medicinal Chemistry*, 21(10):2695–2702, 2013.

[40] Yoshiki Ashida, Ryo C. Yanagita, Yasuhiro Kawanami, Mutsumi Okamura, Shingo Dan, and Kazuhiro Irie. Synthesis, conformation, and biological activities of a des-A-ring analog of 18-deoxy-aplog-1, a simplified analog of debromoaplysiatoxin. *Heterocycles*, 99(2):942–957, 2019.